RAA 2016 Vol. **16** No. **2**, 33 (6pp) doi: 10.1088/1674–4527/16/2/033
http://www.raa-journal.org *http://iopscience.iop.org/raa*

***R**esearch in*
***A**stronomy and*
***A**strophysics*

Three-dimensional orbit and physical parameters of HD 6840

Xiao-Li Wang[1,2], Shu-Lin Ren[1] and Yan-Ning Fu[1]

[1] Purple Mountain Observatory, Chinese Academy of Sciences, Nanjing 210008, China; *rensl@pmo.ac.cn*
[2] University of Chinese Academy of Sciences, Beijing 100049, China

Received 2015 July 14; accepted 2015 August 29

Abstract HD 6840 is a double-lined visual binary with an orbital period of ∼7.5 years. By fitting the speckle interferometric measurements made by the 6 m BTA telescope and 3.5 m WIYN telescope, Balega et al. gave a preliminary astrometric orbital solution of the system in 2006. Recently, Griffin derived a precise spectroscopic orbital solution from radial velocities observed with OPH and Cambridge Coravel. However, due to the low precision of the determined orbital inclination, the derived component masses are not satisfying. By adding the newly collected astrometric data in the Fourth Catalog of Interferometric Measurements of Binary Stars, we give a three-dimensional orbit solution with high precision and derive the preliminary physical parameters of HD 6840 via a simultaneous fit including both astrometric and radial velocity measurements.

Key words: binaries: spectroscopic — astrometry — stars: fundamental parameters — stars: individual (HD 6840)

1 INTRODUCTION

Mass is the most important parameter of a star in deciding its physical state and evolution, and the only reliable way to determine this parameter is determination of a binary orbit requiring two or more types of observational data (Torres et al. 2010). Currently available stellar masses that are measured with high precision are mainly components of double-lined eclipsing binaries, and the physical evolution of these components is seriously influenced by tidal effects (Andersen 1991; Torres et al. 2010). Therefore, precise determination of the component masses in double-lined spectroscopic visual binaries, especially those without close encounters between components, is important for constraining stellar evolutionary models.

Generally speaking, there are no close encounters between components or strong tidal effects in binaries with orbital periods larger than several years. HD 6840 (HIP 5531) is such a system. Its orbital period is ∼ 7.5 years and observational data derived from both its astrometric and spectroscopic measurements are enough to give a precise three-dimensional orbital solution.

Though identified as a visual binary by the Hipparcos mission (ESA 1997), there was only one relative positional datum between the two components provided by Hipparcos. Not long after the publication of the Hipparcos catalog, Horch et al. (1999, 2002) and Balega et al. (2002, 2004, 2006) carried out speckle interferometric measurements. From the resulting tangential position data (TPD), a preliminary astrometric orbital solution of the system was given by Balega et al. (2006). Afterwards, more TPD were provided by Horch et al. (2008, 2009), Balega et al. (2013) and Mason et al. (2009), including those obtained with the adaptive optics instrument Robo-AO (Riddle et al. 2015).

As a double-lined spectroscopic binary, the mass ratio of 0.99 was published in 2004 (Nordström et al. 2004). In 1993, HD 6840 was included in the Cambridge spectroscopic-binary observing program. The long-term radial velocity data (RVD) allowed Griffin (2012) to give a spectroscopic orbital solution with high precision. However, due to the low precision of the determined orbital inclination, the derived component masses are not precise enough to be used in constraining stellar evolutionary models.

In order to give a precise three-dimensional orbital solution, together with the component masses and the orbital parallax, all the above-mentioned observational data coming from different sources should be appropriately weighted and used in a simultaneous fit. To do so, we adopt the weighting scheme by Wang et al. (2015) and apply the fitting method by Ren & Fu (2010).

The observational data that we used are described in Section 2 and the determined three-dimensional orbit is presented in Section 3. Discussions are provided in Section 4.

2 OBSERVATIONAL DATA

2.1 Interferometric Data

Since the first astrometric measurement made by the Hipparcos mission (ESA 1997), HD 6840 has been observed with the speckle interferometric technique by several teams. Horch et al. (1999, 2002) carried out three

speckle interferometric measurements with the Wisconsin-Indiana-Yale-NOAO (WIYN) 3.5 m telescope located at Kitt Peak, Arizona. Using the 6 m BTA telescope of the Special Astrophysical Observatory, Balega et al. (2002, 2004, 2006) made seven speckle interferometric measurements. These measurements lead to 10 TPD, from which a preliminary astrometric orbit solution was given by Balega et al. (2006). Afterwards, 14 more TPD were provided, including seven by Horch et al. (2008, 2009), four by Balega et al. (2013), two by Mason et al. (2009), and one by Riddle et al. (2015) with the adaptive optics instrument Robo-AO.

Extracted from the online version of the Fourth Catalog of Interferometric Measurements of Binary Stars (Hartkopf et al. 2001), the above-mentioned data are listed with their post-fit residuals and associated references in Table 1. In this table, ρ and θ are the polar coordinates of the primary relative to the secondary in the plane of sky with respect to north.

2.2 Spectroscopic Data

In 1993, HD 6840 was included in the Cambridge spectroscopic-binary observing program, and long term RVD of the system were acquired by OPH Coravel and Cambridge Coravel (Griffin 2012). From 1993 to 1998, 19 RVD were obtained by OPH Coravel, and 12 among these RVD were successfully identified as double-lined binaries. In addition, a further 75 RVD were obtained by Cambridge Coravel, and among these, 58 RVD were identified as double-lined cases. By fitting these RVD, a high precision spectroscopic orbital solution was determined by Griffin (2012). Because the RVD of the two component stars cannot be separated spectroscopically, they are not used to fit the orbit in case of error (Griffin 2012) in our work. The RVD that were identified as double-lined cases are listed in Table 2.

3 ORBIT DETERMINATION

For convenience of calculation, the TPD are expressed in rectangular coordinates

$$\begin{aligned} x &= \rho\cos\theta, \\ y &= \rho\sin\theta. \end{aligned}$$

When we use the least squares method to determine the three-dimensional orbit by combining the TPD and the RVD, a simultaneous adjustment of all orbital elements is applied. The objective function is

$$\chi^2 = \sum_{i=1}^{N_1}\left[\left(\frac{x_{\mathrm{o},i}-x_i}{\sigma_{x,i}}\right)^2+\left(\frac{y_{\mathrm{o},i}-y_i}{\sigma_{y,i}}\right)^2\right]+\sum_{j=1}^{N_2}\left[\left(\frac{V_{\mathrm{po},j}-V_{\mathrm{p},j}}{\sigma_{\mathrm{vp},j}}\right)^2+\left(\frac{V_{\mathrm{so},j}-V_{\mathrm{s},j}}{\sigma_{\mathrm{vs},j}}\right)^2\right], \quad (1)$$

where N_1 and N_2 represent the numbers of data points in the TPD and RVD, respectively. The subscript 'o' indicates the observational data, and 'p' and 's' indicate the primary and secondary, respectively. The quantities x, y, V_{p} and V_{s} can be calculated from the orbital elements (Pourbaix 1998).

In Equation (1), the observational data need to be weighted. However, not all the data have known errors. Therefore, post-fit residuals are used to estimate the required errors (Wang et al. 2015). Because the post-fit residual of a datum, namely the difference between the observed and calculated values, depends on model parameters, an iterative process is necessary. Let us first recall this process in the general text. We start with the values of model parameters obtained with the equal weighting scheme. Then the post-residuals can be calculated. For a group of N data observed with the same equipment, we assume a single value for their error, which is simply estimated as the averaged absolute residual

$$\sigma = \sum_{i=1}^{N}\frac{|O_i-C_i|}{N}, \quad (2)$$

where O_i (C_i) is the ith observed (calculated) value. Now the weights of the observational data are well estimated, and so are values in the next iterative step. The iterative process does not stop until the standard errors are all convergent.

The errors of TPD and RVD are calculated separately. Considering the astrometric precision is at about the milliarcsecond (mas) level, when the derived errors are smaller than 1 mas, an error of 1 mas is assumed. After calculation, the errors of the TPD in the declination direction are 1.6, 1.0, 1.4, 4.3 and 4.9 mas for the astrometric data observed by WIYN, BTA, the Hipparcos mission and Robo-AO, and those provided by Mason et al. (2009) respectively, and the corresponding errors of the TPD in the right ascension direction are 2.3, 1.0, 15.0, 1.5 and 1.0 mas. Note that the RVD derived from a close blend are considered as a group of data that is different from the other data for the same component and with the same equipment, and the errors associated with RVD are listed in Table 2.

There are 10 parameters that need to be adjusted, and the modified grid method developed in Ren & Fu (2010) is used to find the global minimum of Equation (1). The determined values of all the parameters including the radial velocity of the barycenter (V_0), the amplitudes of the radial velocity curves (K_1, K_2), the semimajor axis of the relative orbit (a), the inclination (i), the latitude of the ascending node (Ω), the argument of the periastron (ω_A), the eccentricity (e), the period (P), and the time of passage at periastron (T) are given in Table 3, together with the orbital parallax and the component masses (M_1 and M_2). Moreover, the orbital solutions given by Griffin (2012) and Balega et al. (2006) are also listed in the same table for comparison. From this table, we see that the semimajor

Table 1 Astrometric Data of HD 8460

Julian Year	ρ ($''$)	θ ($^\circ$)	$(O-C)_\rho$ ($''$)	$(O-C)_\theta$ ($^\circ$)	Reference
1991.2500	0.136	165.0	0.005	–6.3	ESA (1997)
1997.6300	0.122	162.8	–0.000	0.6	Horch et al. (1999)
1998.7745	0.131	171.9	–0.000	0.0	Balega et al. (2002)
1999.6342	0.125	182.6	0.001	3.5	Horch et al. (2002)
1999.8211	0.121	180.4	–0.000	–0.5	Balega et al. (2004)
2000.7646	0.102	193.3	0.003	1.7	Horch et al. (2002)
2000.8784	0.095	193.1	–0.001	–0.3	Balega et al. (2006)
2002.7960	0.032	310.4	0.006	–2.7	Balega et al. (2006)
2002.7965	0.026	310.0	0.000	–3.3	Balega et al. (2013)
2003.6373	0.065	140.1	0.001	0.6	Horch et al. (2008)
2003.6373	0.065	141.2	0.001	1.7	Horch et al. (2008)
2003.7880	0.075	145.0	0.001	1.1	Balega et al. (2006)
2003.9277	0.082	146.8	–0.000	–0.3	Balega et al. (2013)
2003.9280	0.082	146.8	–0.000	–0.3	Balega et al. (2006)
2004.8155	0.116	159.6	–0.000	0.1	Balega et al. (2007)
2004.8160	0.116	159.5	–0.000	–0.0	Balega et al. (2006)
2005.8625	0.122	167.9	–0.009	–1.0	Mason et al. (2009)
2006.6900	0.129	175.2	0.000	–0.5	Balega et al. (2013)
2007.0093	0.121	177.7	–0.004	–0.7	Horch et al. (2010)
2007.0120	0.127	177.8	0.002	–0.6	Horch et al. (2010)
2007.6049	0.114	184.4	–0.001	0.2	Mason et al. (2009)
2007.8229	0.110	188.2	0.000	1.6	Horch et al. (2010)
2008.6911	0.084	198.7	0.000	–0.9	Horch et al. (2009)
2009.7533	0.039	243.3	–0.001	–0.0	Horch et al. (2012)
2012.7021	0.121	163.6	–0.004	–0.1	Riddle et al. (2015)

axis (a) and the orbital inclination (i) are greatly improved. Then the component masses are two times more precise than those given by Griffin (2012).

The calculated velocity curve and the RVD are shown in Figure 1. The filled circles and open squares with an error bar represent the RVD observed with OPH and Cambridge Coravel, respectively. In addition, the RVD which cannot be used to separate the two components of the system are indicated by open triangles. The apparent orbits given by us and by Balega et al. (2006) are shown in Figure 2 with a solid and dotted ellipse, respectively. Also shown in this figure are the TPD with error bars. The point where the straight dotted lines intersect indicates the periastron. The open circles, squares, triangles, diamond and star with error bars indicate the measurements given by Balega et al. (2002, 2004, 2006, 2013), Horch et al. (1999, 2002, 2012), Mason et al. (2009), Riddle et al. (2015) and Hipparcos mission (ESA 1997), respectively.

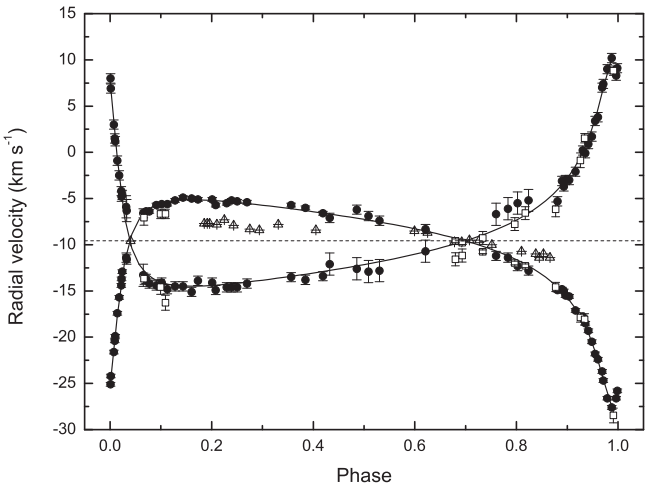

Fig. 1 Radial velocity curve and the RVD. The filled circles and open squares with error bars indicate the RVD obtained with OPH and Cambridge Coravel, respectively. The open triangles represent the RVD which are not used to fit the orbit since these data cannot be used to separate the two components of the system.

4 DISCUSSION

The apparent magnitude in the V band for the system is 6.555 $\pm$ 0.010 (Høg et al. 2000), and the corresponding difference in magnitude between the two components, derived from the average of interferometric observations near the V band (Hartkopf et al. 2001), is about 0.70$\pm$0.1. So, the apparent magnitudes in the V band can be calculated as 7.01$\pm$0.04 and 7.71$\pm$0.07 for the primary and secondary, respectively. Along with the orbital parallax of 16.4$\pm$0.2 mas, we can calculate the absolute magnitudes of the primary and secondary as 3.09$\pm$0.04 and 3.79$\pm$0.07, respectively. Using the color index $(B-V) = 0.0553 \pm 0.005$ from the Hipparcos catalog (van Leeuwen 2007), the bolometric correction can be derived as 0.036$\pm$0.02 (Flower 1996). Then, the luminosities can be derived as 4.78$\pm$0.20 and 2.51$\pm$0.17 for the primary and secondary, respectively.

Table 2 Radial Velocity Data of HD 6840

MJD	RV_p (m s^{-1})	σ_p (km s^{-1})	$(O-C)$ (km s^{-1})	RV_s (km s^{-1})	σ_s (km s^{-1})	$(O-C)$ (km s^{-1})	Equipment
49028.810(*)	–8.9	0.2	0.1	–10.9	0.7	–1.2	OPH Coravel
49064.780(*)	–9.1	0.2	0.1	–10.5	0.7	–1.0	OPH Coravel
49176.110(*)	–10.1	0.2	–0.2	–8.6	0.7	0.1	OPH Coravel
49346.890(*)	–11.3	0.2	0.0	–7.1	0.7	0.1	OPH Coravel
49402.770(*)	–11.6	0.2	0.2	–5.9	0.7	0.7	OPH Coravel
49566.110	–13.9	0.5	0.2	–5.5	0.8	–1.4	OPH Coravel
49698.840	–17.2	0.5	0.3	–0.2	0.8	0.1	OPH Coravel
49720.790	–17.4	0.6	1.0	2.2	0.5	1.6	OPH Coravel
49875.120	–27.8	0.8	–0.6	9.5	0.5	–0.9	OPH Coravel
50082.830	–6.4	0.8	0.0	–13.0	0.6	–0.4	OPH Coravel
50171.790	–6.0	0.5	–0.7	–13.9	0.8	–0.1	OPH Coravel
50197.830	–6.0	0.5	–0.8	–15.6	0.8	–1.7	OPH Coravel
52298.850	–14.9	0.2	–0.4	–5.3	0.5	–1.2	Cambridge Coravel
52321.820	–14.8	0.2	0.2	–3.1	0.5	0.5	Cambridge Coravel
52340.820	–15.5	0.2	–0.1	–3.0	0.5	0.1	Cambridge Coravel
52448.080	–18.5	0.2	0.3	–0.1	0.5	–0.7	Cambridge Coravel
52482.090	–20.5	0.2	–0.1	1.7	0.5	–0.7	Cambridge Coravel
52515.120	–22.4	0.2	0.1	3.8	0.5	–0.8	Cambridge Coravel
52544.070	–24.7	0.2	–0.1	7.4	0.5	0.4	Cambridge Coravel
52565.050	–26.6	0.2	–0.4	9.0	0.5	0.3	Cambridge Coravel
52588.980	–27.6	0.2	–0.2	10.2	0.5	0.1	Cambridge Coravel
52612.940	–26.6	0.2	0.0	8.3	0.5	–0.9	Cambridge Coravel
52619.070	–25.8	0.2	0.1	9.1	0.5	0.7	Cambridge Coravel
52625.760	–25.1	0.2	–0.2	8.0	0.5	0.6	Cambridge Coravel
52627.820	–24.2	0.2	0.4	6.9	0.5	–0.1	Cambridge Coravel
52643.760	–21.6	0.2	–0.2	3.0	0.5	–0.5	Cambridge Coravel
52650.870	–19.9	0.2	0.0	1.2	0.5	–0.6	Cambridge Coravel
52662.870	–17.4	0.2	0.1	-0.9	0.5	-0.1	Cambridge Coravel
52671.800	–15.7	0.2	0.2	–2.5	0.5	0.1	Cambridge Coravel
52683.850	–14.4	0.2	–0.4	–4.2	0.5	0.5	Cambridge Coravel
52688.860	–12.9	0.2	0.4	–4.6	0.5	0.9	Cambridge Corvael
52712.790(*)	–11.6	0.5	–0.8	–6.3	1.2	2.0	Cambridge Coravel
52801.080(*)	–6.6	0.5	0.1	–13.3	1.2	–0.6	Cambridge Coravel
52834.090	–6.4	0.2	–0.3	–14.2	0.5	–0.9	Cambridge Coravel
52871.110	–5.7	0.2	0.0	–14.4	0.5	–0.6	Cambridge Coravel
52900.120	–5.6	0.2	–0.1	–14.1	0.5	–0.1	Cambridge Coravel
52930.030	–5.6	0.2	–0.2	–14.8	0.5	–0.6	Cambridge Coravel
52970.940	–5.2	0.2	0.0	–14.5	0.5	–0.2	Cambridge Coravel
53013.790	–4.9	0.2	0.3	–14.5	0.5	–0.1	Cambridge Coravel
53060.830	–5.0	0.2	0.2	–15.1	0.5	–0.7	Cambridge Coravel
53189.090	–5.7	0.2	–0.4	–14.9	0.5	–0.6	Cambridge Coravel
53248.070	–5.5	0.2	–0.2	–14.6	0.5	–0.4	Cambridge Coravel
53274.070	–5.2	0.2	0.2	–14.6	0.5	–0.4	Cambridge Coravel
53304.010	–5.3	0.2	0.1	–14.6	0.5	–0.5	Cambridge Coravel
53356.880	–5.4	0.2	0.1	–14.2	0.5	–0.2	Cambridge Coravel
53593.130	–5.7	0.2	0.4	–13.5	0.5	–0.1	Cambridge Coravel
53669.990	–6.0	0.2	0.3	–13.8	0.5	–0.6	Cambridge Coravel
53763.780	–6.6	0.2	0.0	–13.4	0.5	–0.5	Cambridge Coravel
53800.790(*)	–7.1	0.5	–0.4	–12.1	1.2	0.7	Cambridge Coravel
53945.130(*)	–6.2	0.5	0.9	–12.6	1.2	–0.3	Cambridge Coravel
54008.110(*)	–6.9	0.5	0.4	–12.9	1.2	–0.9	Cambridge Coravel
54067.000(*)	–7.4	0.5	0.1	–12.8	1.2	–1.0	Cambridge Coravel
54313.120(*)	–8.3	0.5	0.2	–10.7	1.2	0.1	Cambridge Coravel
54691.140(*)	–11.2	0.5	–0.6	–6.7	1.2	1.7	Cambridge Coravel
54756.000(*)	–11.4	0.5	–0.2	–6.1	1.2	1.7	Cambridge Coravel
54806.990(*)	–12.3	0.5	–0.7	–5.5	1.2	1.8	Cambridge Coravel
54865.800(*)	–12.8	0.5	–0.5	–5.2	1.2	1.4	Cambridge Coravel
55055.110	–15.0	0.2	0.3	–3.7	0.5	–0.4	Cambridge Coravel
55084.100	–15.6	0.2	0.3	–3.0	0.5	–0.5	Cambridge Coravel
55117.010	–17.1	0.2	–0.2	–2.1	0.5	–0.6	Cambridge Coravel
55155.960	–17.8	0.2	0.4	0.2	0.5	0.2	Cambridge Coravel
55185.870	–19.3	0.2	0.2	0.9	0.5	–0.5	Cambridge Coravel
55222.780	–21.8	0.2	–0.3	3.4	0.5	–0.2	Cambridge Coravel
55259.810	–23.7	0.2	0.4	7.0	0.5	0.6	Cambridge Coravel
55371.090	–20.4	0.2	0.0	1.5	0.5	–0.8	Cambridge Coravel
55407.120	–13.7	0.2	0.2	–4.8	0.5	0.0	Cambridge Coravel
55432.140(*)	–11.4	0.5	–0.4	–5.9	1.2	2.1	Cambridge Coravel
55538.960	–6.4	0.2	0.0	–13.7	0.5	–0.7	Cambridge Coravel
55817.070	–5.1	0.2	0.1	–13.9	0.5	0.5	Cambridge Coravel
55892.950	–5.1	0.2	0.1	–14.1	0.5	0.3	Cambridge Coravel

Notes: (*) The RV data are derived from close blends.

Table 3 The Newly Derived and Historical Orbital Parameters and Masses of HD 8640

Parameter	The present work	Griffin (2012)	Balega et al. (2006)
V_0 (km s^{-1})	–9.57±0.03	–9.57±0.04	
K_1 (km s^{-1})	11.16 ± 0.05	11.18±0.06	
K_2 (km s^{-1})	12.30 ± 0.09	12.34±0.12	
ω_A (°)	215.6±0.3	215.2 ± 0.5	219.1±1.4
e	0.7433±0.0014	0.7442 ± 0.0020	0.720±0.008
P (d)	2722.4±0.7	2722.0±1.0	2666±40
T (JD-2400000.5)	52622.6±0.6	52622.2±0.9	49976±40
a (mas)	83.0±0.3		87±2
i (°)	50.9±0.5		54.7±1.5
Ω (°)	151.3±0.3		151.6±1.3
Orbital parallax (mas)	16.4±0.2		
M_1 ($M_\odot$)	1.22±0.03	1.06±0.06	
M_2 ($M_\odot$)	1.11±0.03	0.96±0.06	

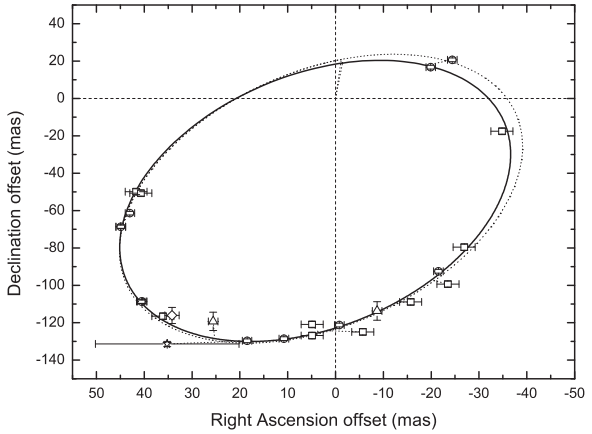

Fig. 2 Apparent orbit and the astrometric data of HD 6840. The solid ellipse is the newly derived apparent orbit and the dotted one is derived from Balega et al. (2006).

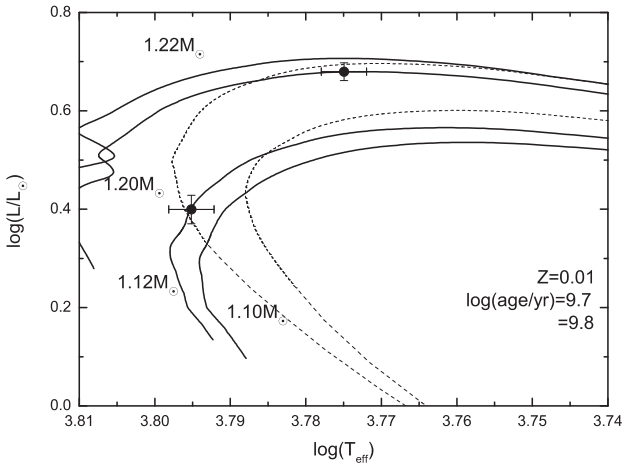

Fig. 3 Evolutionary tracks and isochrones for the two component stars of HD 6840 (Mowlavi et al. 2012). The solid lines and dashed lines indicate the mass tracks of 1.10, 1.12, 1.20 and 1.22 $M_\odot$ and the isochrones of $\log$ (age yr^{-1}) $= 9.7$ and 9.8, respectively.

The effective temperature of 5956±35 K for the system was given by Ramírez et al. (2012, 2013). Considering the effective temperature of the system as that of the primary, we attempt to investigate the evolutionary status by comparing the ($\log T_{\rm eff}$, $\log L/L_\odot$) values of the component stars with the evolutionary model given by Mowlavi et al. (2012). We find that the primary is on the horizontal branch of the Hertzsprung-Russell diagram, so the mass and age of the primary are hardly influenced by the effective temperature. Then, we find a good match between the observation and evolutionary model with metallicity $Z = 0.01$ (Mowlavi et al. 2012). The tracks representing masses 1.10, 1.12, 1.20 and 1.22 $M_\odot$ are shown by the solid lines in Figure 3, and the isochrones for $\log(\text{age yr}^{-1}) = 9.7$ and 9.8 are also shown by the dashed lines in the same figure.

From Figure 3, the logarithm of the isochrone age of about 9.71 can be inferred, and the temperature of the secondary can be derived as 6240±35 K by the same isochrone age as the primary. Although we have found a good match between the observation and model with the value of metallicity $Z = 0.01$, the value $Z = 0.01$ is slightly different from the observation of [Fe/H]$= -0.38$ corresponding to $Z = 0.0053$ (Ramírez et al. 2012, 2013).

In this work, we obtain the three-dimensional orbit of the system HD 6840 and preliminarily analyze the properties of its components by the stellar evolutionary model. In order to improve the precision of the orbit, interferometric observations are still needed to cover the whole orbit. On the other hand, in order to obtain the model-independent physical properties and test the stellar evolutionary model, high resolution and high signal-to-noise spectral observations are also needed and the composite spectra of the system are expected to be disentangled in the future.

Acknowledgements This research has made use of the SIMBAD astronomical literature database, operated at CDS, Strasbourg, France. We would like to thank an anonymous referee for his or her many instructive remarks. This research is supported by the National Natural Science Foundation of China (Grant Nos. 11073059, 10833001, 11178006, 11273066 and 11203086).

References

Andersen, J. 1991, A&A Rev., 3, 91
Balega, I. I., Balega, Y. Y., Hofmann, K.-H., et al. 2002, A&A, 385, 87
Balega, I., Balega, Y. Y., Maksimov, A. F., et al. 2004, A&A, 422, 627
Balega, I. I., Balega, Y. Y., Hofmann, K.-H., et al. 2006, A&A, 448, 703
Balega, I. I., Balega, Y. Y., Maksimov, A. F., et al. 2007, Astrophysical Bulletin, 62, 339
Balega, I. I., Balega, Y. Y., Gasanova, L. T., et al. 2013, Astrophysical Bulletin, 68, 53
ESA, ed. 1997, ESA Special Publication, 1200, The HIPPARCOS and TYCHO Catalogues. Astrometric and Photometric Star Catalogues Derived from the ESA HIPPARCOS Space Astrometry Mission
Flower, P. J. 1996, ApJ, 469, 355
Griffin, R. F. 2012, The Observatory, 132, 309
Hartkopf, W. I., McAlister, H. A., & Mason, B. D. 2001, AJ, 122, 3480
Høg, E., Fabricius, C., Makarov, V. V., et al. 2000, A&A, 355, L27
Horch, E., Ninkov, Z., van Altena, W. F., et al. 1999, AJ, 117, 548
Horch, E. P., Robinson, S. E., Meyer, R. D., et al. 2002, AJ, 123, 3442
Horch, E. P., van Altena, W. F., Cyr, Jr., W. M., et al. 2008, AJ, 136, 312
Horch, E. P., Veillette, D. R., Baena Gallé, R., et al. 2009, AJ, 137, 5057
Horch, E. P., Falta, D., Anderson, L. M., et al. 2010, AJ, 139, 205
Horch, E. P., Bahi, L. A. P., Gaulin, J. R., et al. 2012, AJ, 143, 10
Mason, B. D., Hartkopf, W. I., Gies, D. R., Henry, T. J., & Helsel, J. W. 2009, AJ, 137, 3358
Mowlavi, N., Eggenberger, P., Meynet, G., et al. 2012, A&A, 541, A41
Nordström, B., Mayor, M., Andersen, J., et al. 2004, A&A, 418, 989
Pourbaix, D. 1998, A&AS, 131, 377
Ramírez, I., Allende Prieto, C., & Lambert, D. L. 2013, ApJ, 764, 78
Ramírez, I., Fish, J. R., Lambert, D. L., & Allende Prieto, C. 2012, ApJ, 756, 46
Ren, S., & Fu, Y. 2010, AJ, 139, 1975
Riddle, R. L., Tokovinin, A., Mason, B. D., et al. 2015, ApJ, 799, 4
Torres, G., Andersen, J., & Giménez, A. 2010, A&A Rev., 18, 67
van Leeuwen, F., ed. 2007, Astrophysics and Space Science Library, 350, Hipparcos, the New Reduction of the Raw Data
Wang, X., Hummel, C. A., Ren, S., & Fu, Y. 2015, AJ, 149, 110